 CMES, vol.67, no.3, pp.175-209, 2010

Molecular Dynamics Analysis of the Vaporization Process for Two Nano-Scale Liquid Threads Coexisting in a Periodic Fundamental Cell

Chun-Lang Yeh[1]

Abstract: Previous studies of nano-scale liquid threads have almost entirely been devoted to the investigation of a single liquid thread in a periodic fundamental cell. This paper is the first to study the vaporization process of two nano-scale liquid threads coexisting in a periodic fundamental cell by molecular dynamics (MD) simulation. Because of the interaction between the two liquid threads, the vaporization process is different from that of a single liquid thread in a periodic fundamental cell. This study discusses the influences of the liquid thread radius, fundamental cell length, and relative position of the two threads. Snapshots of molecules, the number of liquid particles formed, and density field are analyzed. Two linear stability criteria, namely, Rayleigh's stability criterion and Kim's stability criterion, are accessed for their validity in molecular scale. It is found that the two liquid threads may remain intact or evolve into only one liquid particle if the fundamental cell length is small. If the threads break up in this case, they rupture from their ends only, i.e. the top and bottom surfaces of the fundamental cell, but not from their interiors. On the other hand, if the fundamental cell length is larger, more than one liquid particle may be produced in the cell and the liquid threads rupture not only from their ends but also from their interiors. It is also found that thinner liquid threads may produce more liquid particles in the cell and evaporate more quickly. In addition, more liquid particles are formed when the separation of the two threads is larger. Moreover, vaporization is slower when the two liquid threads are close to each other. On the basis of identical liquid thread radius and length, liquid threads that produce more liquid particles evaporate more quickly. Finally, the trends of Rayleigh's stability criterion and Kim's stability criterion agree with MD simulation results. However, when the two threads coalesce into a single thread and remain intact, the critical wavelength of perturbation may be increased and the stable domain is broadened. Under such a situation, Rayleigh's stability criterion and Kim's stability criterion underpredict the stable domain.

[1] Department of Aeronautical Engineering, National Formosa University, Huwei, Yunlin 632, Taiwan, R.O.C.Tel. No.: 886-5-6315527, Fax No.: 886-5-6312415, E-mail: clyeh@nfu.edu.tw

Keywords: Coexisting Nano-Scale Liquid Threads, Molecular Dynamics Simulation, Rayleigh's stability criterion, Kim's stability criterion

Nomenclature

k_B	Boltzmann constant
L	fundamental cell length
m	molecular mass
N	number of molecules
Np	number of liquid particles produced in the fundamental cell
R	liquid thread radius
r	intermolecular distance
r_c	cut-off radius of Lennard-Jones potential function
T	temperature
t	time
Δt	time step
V	volume
v_i	velocity of molecule i
x, y, z	Cartesian coordinates

Greek

ε	energy parameter of Lennard-Jones potential function
ρ	density
σ	length parameter of Lennard-Jones potential function
ϕ	Lennard-Jones potential function

Subscripts

L	liquid phase
V	vapor phase

Superscripts

*	non-dimensionalized quantity
_	averaged quantity

1 Introduction

The formation of liquid threads is one of the most fundamental and important phenomena during the atomization process. In our previous studies [Yeh (2005, 2009a)] of atomizer flow, it can be seen that the liquid evolves into threads after leaving the atomizer. Previous studies of nano-scale liquid threads have mostly been devoted to the investigation of a single liquid thread in a periodic fundamental cell. Lord Rayleigh (1879) analyzed the instability of an inviscid liquid cylinder and a viscous one. Later on, Weber (1931) and Tomotika (1935) considered more realistic cases of liquid threads in unbounded domains. Goren (1962) studied the annular thread of fluid in contact with a solid. He used linear stability analysis to determine the fastest growing mode when either inertia or viscous forces are negligible. Koplik and Banavar (1993) studied the Rayleigh's instability of a cylindrical liquid thread in a vacuum by using a three-dimensional molecular dynamics (MD) simulation. The maximum number of molecules they used consisted of 8,192 liquid argon Lennard-Jones molecules for a cylindrical liquid thread with a non-dimensionalized radius of 7.5 in a box with a non-dimensionalized length of 54.7. For this simulation condition, only one liquid particle was formed. When a smaller computational domain was used instead, no liquid particle was found in their study. Kawano (1998) applied 10,278 Lennard-Jones molecules of liquid and vapor coexisting argon in three dimensions to analyze the interfacial motion of a cylindrical liquid thread with a non-dimensionalized radii of 2.0 to 4.0 in a box with a non-dimensionalized length up to 120. For this kind of condition with a larger computational domain, a maximum number of 8 to 9 liquid particles were observed. Min and Wong (2006) studied the Rayleigh's instability of nano-scale Lennard-Jones liquid threads by MD simulation and concluded that Rayleigh's continuum prediction holds down to the molecular scale. Kim, Lee, Han and Park (2006) applied MD simulation to investigate the thermodynamic properties and stability characteristics of a nano-scale liquid thread. They found that the overall trends of the simulation results agree with classical stability theory. However, classical theory overpredicts the region of stable domain as the radius decreases compared to the MD results.

Establishing a nano-scale system is still a complex task because of the major challenges in fabricating the nano-locating and nano-driving assemblies. On the other hand, MD can offer novel insights into the underlying atomistic mechanisms and nano-scale behavior due to their high temporal and spatial resolution. Liu and Tsai (2009) proposed a numerical method for extracting the thermo-mechanical properties of a thin-film. In their study, MD simulations were utilized to establish the load-displacement response of a thin copper substrate. Chen, Cheng and Hsu (2007) evaluated the fundamental mechanical properties of single/multi-walled carbon nano-tubes (CNTs) using MD simulations. In their study, the force field be-

tween two carbon atoms is modeled with the Tersoff-Brenner potential while the inlayer/interlayer van der Waals (vdW) atomistic interactions are simulated with the Lennard-Jones potential. They found that the effect of the inlayer vdW atomistic interactions cannot be neglected and should receive attention in MD simulations of the mechanical properties of CNTs. Matsumoto, Nakagaki, Nakatani and Kitagawa (2005) studied the internal structure-changes around the crack tip and the pertinent crack growth behavior in an amorphous metal by MD simulation. The Finnis-Sinclair potential for α-iron was used to describe the inter-atomic potential. The computed results showed that nano-scale crystalline phase grows around the crack tip and that the distribution of deformation zones and deformation mechanisms are significantly altered.

As mentioned above, previous studies of nano-scale liquid threads have mostly been devoted to the investigation of a single liquid thread in a periodic fundamental cell. This study is the first to investigate the vaporization process of two nano-scale liquid threads coexisting in a periodic fundamental cell by MD simulation. Because of the interaction between the two nano-scale liquid threads coexisting in a periodic fundamental cell, the vaporization process is different from that of a single liquid thread in a periodic fundamental cell. This study discusses the influences of the liquid thread radius, fundamental cell length, and relative position of the two threads. Snapshots of molecules, the number of liquid particles formed, and density field are analyzed. Two linear stability criteria, namely, Rayleigh's stability criterion and Kim's stability criterion, are accessed for their validity in molecular scale. This approach will be helpful for the understanding and prediction of the atomization process.

2 Molecular Dynamics Simulation Method

In this study, the vaporization process of the liquid threads is investigated by MD simulation. The inter-atomic potential is one of the most important parts of MD simulation. Many potential models exist, such as hard sphere, soft sphere, square well, and so on [Haile (1992)]. In this study, the Lennard-Jones 12-6 potential model, which is widely used, is adopted for calculation. It is

$$\phi(\mathrm{r}) = 4\varepsilon \left[\left(\frac{\sigma}{r} \right)^{12} - \left(\frac{\sigma}{r} \right)^{6} \right] \tag{1}$$

where r denotes the distance between two molecules and ε and σ are the representative scales of energy and length, respectively. The Lennard-Jones fluid in this study is taken to be argon due to its ease of physical understanding. The parameters for argon are as follows [Kawano (1998)] : the length parameter σ=0.354 nm, the energy parameter ε/k_B=93.3K, and the molecular weight m=6.64$\times 10^{-26}$ kg, where

k_B=1.38×10^{-23} J/K denotes the Boltzmann constant. The cut-off radius r_c beyond which the intermolecular interaction is neglected is 5.0σ.

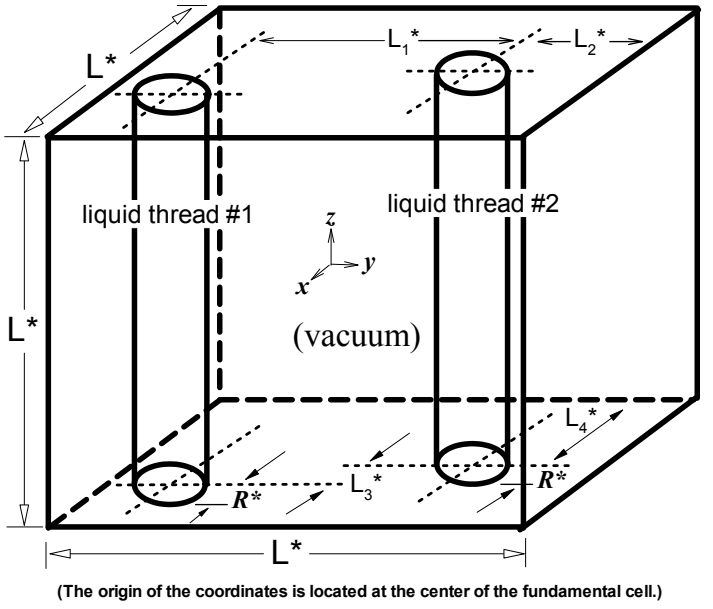

Figure 1: Illustration of the computational domain for the simulation of two nano-scale liquid threads coexisting in a periodic fundamental cell

The simulation domain is schematically shown in Fig.1, with periodic boundary conditions applied in all three directions. Simulation domain dimensions, the relative position of the two threads and number of molecules are listed in Table 1, together with some simulation results. Note that in Table 1, the number in the parenthesis in the Np column denotes the number of liquid particles formed at time t*=1000, while the number outside the parenthesis in the Np column denotes the maximum number of liquid particles formed during the vaporization process. If no parenthesis is denoted, it means that the maximum number of liquid particles formed prevails over the vaporization process. The time integration of motion is performed by Gear's fifth predictor-corrector method [Haile (1992)] with a time step of t^*=0.001 (i.e. 2.5 fs) . Note that all quantities with an asterisk in this study, such as L*, R^*, ρ^*, t^*, etc., are non-dimensionalized in terms of σ, ε, and m, i.e. L^*=L/σ, R^*=R/σ, ρ^*=$N\sigma^3$/V, $t^* = t\ (\varepsilon/m)^{1/2}/\sigma$, $T^* = k_B T/\varepsilon$.

In this study, two cylindrical liquid threads of length L^* and radius R^* are placed in the computational domain and the remaining space is a vacuum. The relative position of the two threads is controlled by L_1^*, L_2^* and L_4^*, as shown in Fig.1. L_3^*

Table 1: Simulation domain dimensions, relative position of the two threads, number of molecules, and simulation results (L_3^*=0)

Case No.	Corresponding Figure No.	R*	L*	L_1^*	L_2^*	L_4^*	N_{mol}	$\overline{f_\rho}$	Np
1	2	4	30	10	10	15	2450	0.649	0
2	3	2	30	10	10	15	606	0.465	2(1)†
3	4	4	60	30	15	30	4934	0.633	2
4	5	4	60	10	25	30	4934	0.683	1
5		4	60				2467	0.652	1
6	6	2	60	30	15	30	1276	0.519	2
7	7	2	60	10	25	30	1276	0.614	2(1)
8		2	60				638	0.542	1
9	8	4	120	60	30	60	9886	0.706	2
10	9	4	120	40	40	60	9886	0.708	2
11	10	4	120	10	55	60	9886	0.745	1
12		4	120				4943	0.741	1
13	11	2	120	60	30	60	2442	0.531	10(2)
14	12	2	120	40	40	60	2442	0.539	9(2)
15	13	2	120	10	55	60	2442	0.568	9(1)
16		2	120				1221	0.635	2(1)
17	14	4	240	120	60	120	19734	0.807	2
18	15	4	240	40	100	120	19734	0.811	2
19	16	4	240	10	115	120	19734	0.824	1
20		4	240				9867	0.839	1
21	17	4	480	160	160	240	39418	0.829	8(4)
22	18	4	480	40	220	240	39418	0.847	6(2)
23	19	4	480	10	235	240	39418	0.875	2(1)
24		4	480				19709	0.857	3(1)

† The number in the parenthesis in the Np column denotes the number of liquid particles formed at time t*=1000, while the number outside the parenthesis in the Np column denotes the maximum number of liquid particles formed during the vaporization process. If no parenthesis is denoted, it means that the maximum number of liquid particles formed prevails over the vaporization process.

is set to be zero, i.e., the two liquid threads are kept at x=0 initially and are shifted only in the y direction. The initial density of the liquid argon is ρ_L^*=0.819 and the system temperature is kept at T^*=0.75. These dimensionless values correspond to ρ_L=1223 kg/m^3 for argon and T=70K, which is below the critical temperature (150K) of argon.

The procedure for MD simulation includes three stages : initialization, equilibration and production. Initially, equilibration is performed for liquid argon molecules in a rectangular parallelepiped with length and width equal to the liquid thread diameter (D^*=2R^*=4 or 8) and with height equal to the side length of the computational domain (L^*=30, 60, 120, 240, 480). The initial velocities of molecules are decided by normal random numbers. Velocity rescaling is performed at each time step by Eq.(2) to make sure that the molecules are at the desired temperature T^* :

$$v_i^{new} = v_i^{old} \sqrt{\frac{T_D}{T_A}} \tag{2}$$

where v_i^{old} and v_i^{new} are the velocities of molecule i before and after correction, respectively, and T_D and T_A are the desired and the actual molecular temperatures, respectively. The liquid molecules are equilibrated for 10^6 time steps at the desired temperature T^*. The achievement of an equilibrium state is confirmed by obtaining the radial distribution function. After the liquid molecules are equilibrated, the rectangular parallelepiped for the liquid molecules is truncated to the desired cylindrical liquid thread by removing unwanted regions. The cylindrical liquid threads are then put into the computational domain and the production stage proceeds. A minimum image method and the Verlet neighbor list scheme [Haile (1992)] to keep track of which molecules are actually interacting at a given time interval of 0.005 are used in the equilibration and the production stages.

In practical applications, e.g., combustors or printers, faster vaporization is usually desirable. Criteria have to be made to quantify the discussion regarding the vaporization process of a liquid thread. In this study, a liquid thread is considered to vaporize faster if the distribution of molecules reaches uniform state more quickly during the vaporization process. This criterion essentially is concerned with the evolution of the density distribution. The density at a specified point in the fundamental cell can be defined as

$$\rho = \lim_{\delta V \to 0} \frac{\delta N}{\delta V} \tag{3}$$

where δV is a small volume surrounding the point considered and δN is the number of molecules inside the volume δV. The density defined by Eq.(3) is actually an averaged density of the small volume surrounding the point considered. The

value will approach the density of a specified point if the volume δV shrinks to that point. However, for a meaningful density field, the volume δV cannot be too small because when δV becomes too small, it is difficult to obtain a definite value for $\delta N/\delta V$. In this study, the volume δV is taken to be a sphere with non-dimensionalized radius R^*=2 and with its center located at the point considered. This is an optimal choice after numerical testing.

The time averaged density uniformity factor, $\overline{f_\rho}$, in a time interval of $t*$=0 to 1000, as listed in Table 1, can be used to indicate the vaporization speed of the liquid threads. The density uniformity factor, f_ρ , is defined as

$$f_\rho = \frac{\sum_N \left(\rho^* - \rho^*_{eq}\right)_{t^*} \Delta V}{\sum_N \left(\rho^* - \rho^*_{eq}\right)_{t^*=0} \Delta V} \tag{4}$$

where N is the total number of molecules in the fundamental cell, i.e., N_{mol} in Table 1, ρ^* and ΔV are the density and volume of molecule i, respectively, as defined by Eq.(3), and ρ^*_{eq} is the density value when the molecules are uniformly distributed, i.e. $\rho^*_{eq} \equiv N_{mol}$/ Vol, where Vol is the volume of the fundamental cell. The density uniformity factor, f_ρ , as defined by Eq.(4), represents the deviation from uniform state. A smaller time averaged density uniformity factor, $\overline{f_\rho}$, implies that the distribution of liquid thread molecules reaches uniform state more quickly during the vaporization process and therefore represents faster vaporization.

3 Results and Discussions

In the following discussion, two cylindrical liquid threads of length L^* and radius R^* are placed in the computational domain and the remaining space is a vacuum. The relative position of the two threads is controlled by L^*_1, L^*_2 and L^*_4, as shown in Fig.1. Simulation domain dimensions and the number of molecules are listed in Table 1.

3.1 Liquid Thread Vaporization Process

Figure 2 shows the vaporization process of two liquid threads of R^*=4, L^*=30, L^*_1=10, L^*_2=10 and L^*_4=15 (case 1 in Table 1) . Note that L^*=30 and R^*=4 correspond to L=10.6nm and R=1.41nm, respectively. It can be seen that the two liquid threads quickly coalesce into a single thread and remain intact. No liquid particles are formed during the vaporization process. Figure 3 shows the vaporization process of two liquid threads of smaller radius R^*=2 but with the same length and relative position : L^*=30, L^*_1=10, L^*_2=10 and L^*_4=15 (case 2 in Table 1) . For this case in which the liquid threads are thinner, it is seen that the two threads rupture from their two ends, i.e., the top and bottom surfaces of the fundamental cell, and

get shorter due to the contraction motion in their axial directions. Two liquid particles are formed and they quickly coalesce into a single particle by collision and coalescence. The coalesced liquid particle prevails during the subsequent vaporization process.

From Table 1, it is seen that the value of $\overline{f_\rho}$ is smaller for the thinner liquid threads. As stated in the previous section, this implies that the thinner liquid threads evaporate more quickly. In addition, it can be seen from Table 1 that the thinner liquid threads produce more liquid particles. In our previous study (2009b), we found that a single liquid thread is more unstable and produces more liquid particles when it is thinner. The present results for two liquid threads coexisting in a fundamental cell corroborate the findings of the previous study of a single liquid thread.

Figure 4 shows the vaporization process of two liquid threads of R^*=4, L^*=60, L_1^*=30, L_2^*=15 and L_4^*=30 (case 3 in Table 1) . It is observed that the two threads rupture from their two ends, i.e., the top and bottom surfaces of the fundamental cell, and get shorter due to the contraction motion in their axial directions. Two liquid particles are formed and prevail during the subsequent vaporization process. In contrast to cases 1 and 2 for shorter liquid threads, the two liquid particles do not coalesce. If the two liquid threads get closer to each other, e.g., R^*=4, L^*=60, L_1^*=10, L_2^*=25 and L_4^*=30 (case 4 in Table 1) , the vaporization process, which is shown in Fig.5, would be very different from case 3. From Fig.5, it is seen that because the two threads are very close to each other, they quickly coalesce into a single thread. The coalesced liquid thread gets shorter due to the contraction motion in its axial direction and finally evolves into a single liquid particle.

From Table 1, it can be seen that the value of $\overline{f_\rho}$ is larger for case 4. This implies that vaporization is slower when the two liquid threads are close to each other. In addition, Table 1 shows that more liquid particles are formed when the separation of the two threads is larger (case 3 in Table 1) . In our previous study (2009b), we found that molecular interaction plays an important role in the vaporization process. More liquid particles can provide more molecular interactions, which is conducive to vaporization. Comparison of cases 3, 4 and 5 also reveals this tendency. Case 5, which was investigated in our previous study (2009b), denotes the situation for a single liquid thread of the same radius and length as in cases 3 and 4. From Table 1, it is observed that only one liquid particle is formed for case 5 and the vaporization speed for case 5 is slower than case 3, for which two liquid particles are formed. The present results for two liquid threads coexisting in a fundamental cell corroborate the findings of our previous study for a single liquid thread.

Figure 6 shows the vaporization process of two liquid threads of R^*=2, L^*=60, L_1^*=30, L_2^*=15 and L_4^*=30 (case 6 in Table 1) . Similar to case 3, the two threads rupture from their two ends and get shorter due to the contraction motion in their

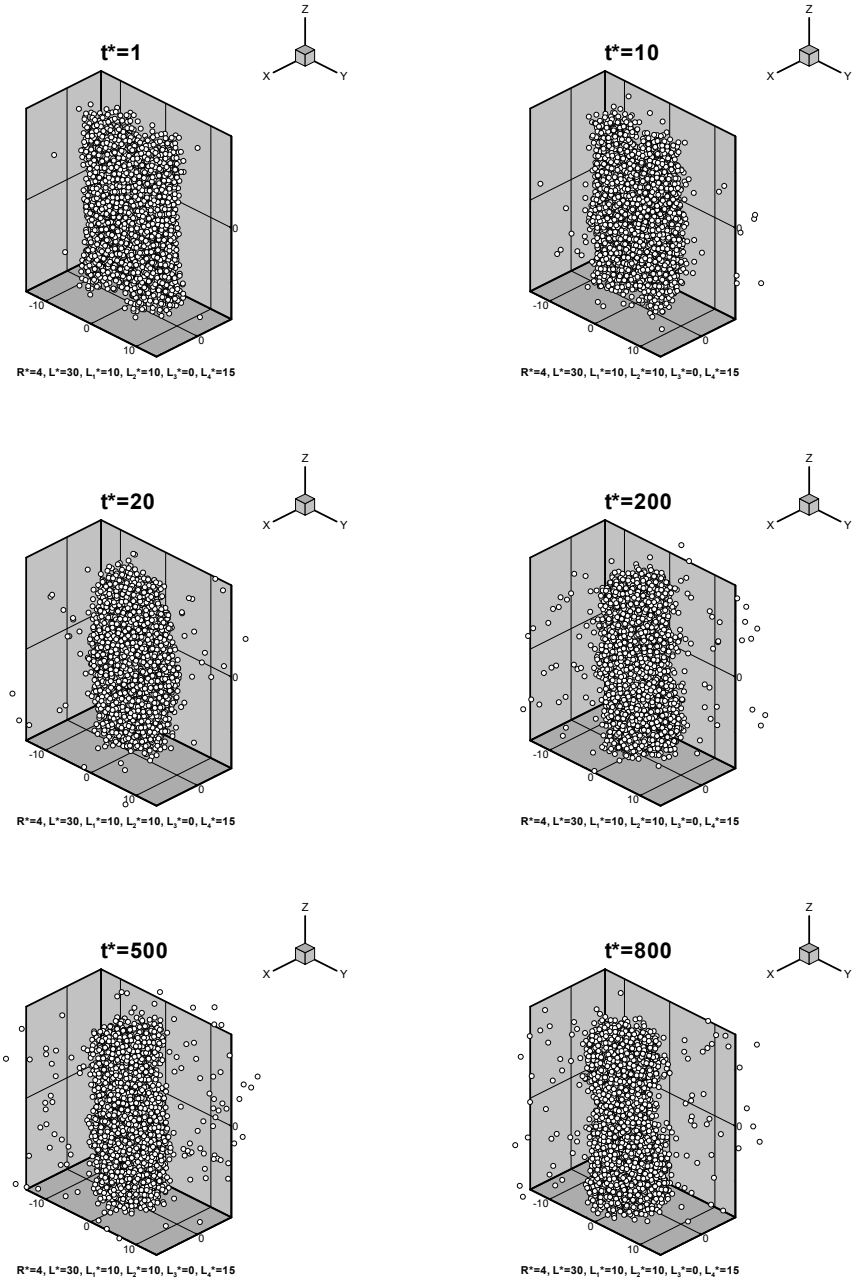

Figure 2: Vaporization process of two liquid threads of R^*=4, L^*=30, L_1^*=10, L_2^*=10, L_3^*=0, L_4^*=15

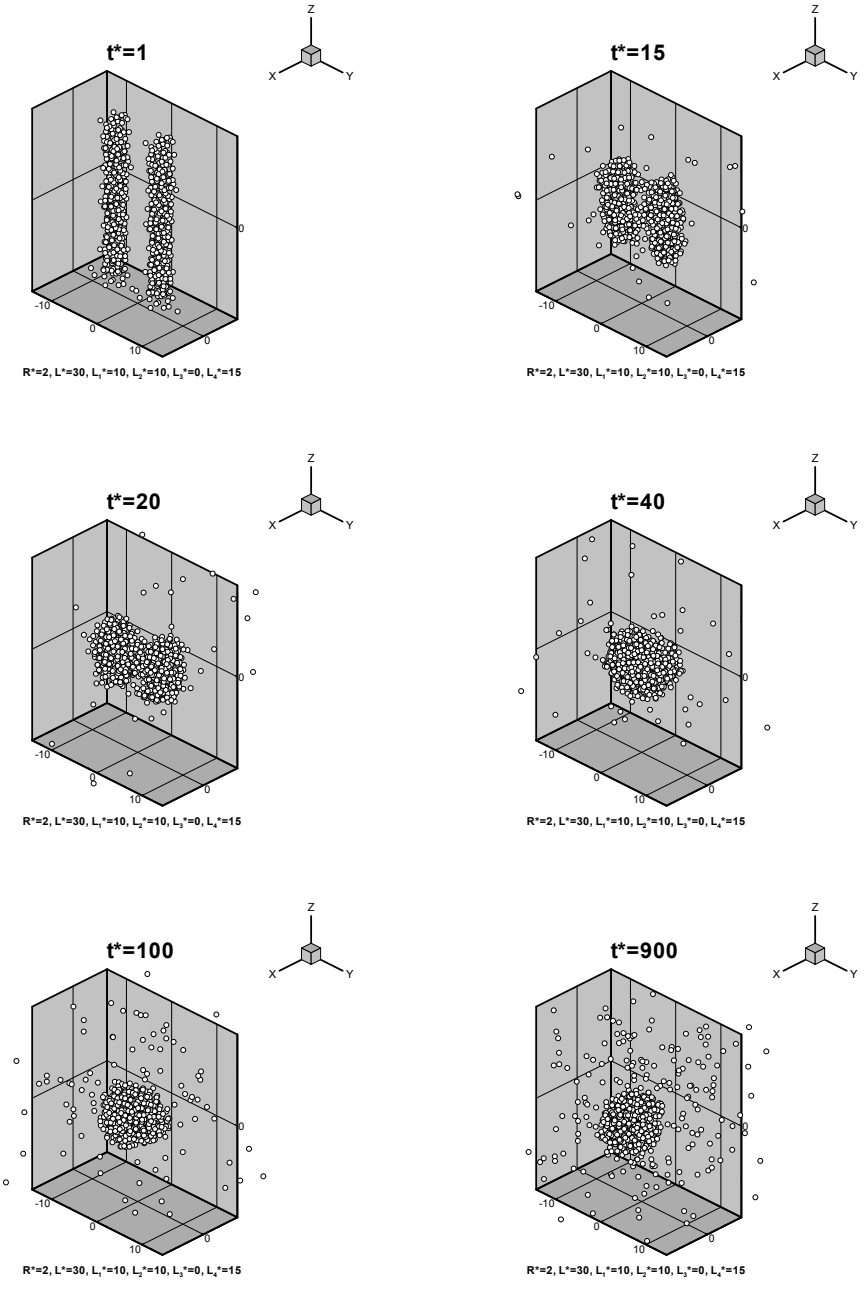

Figure 3: Vaporization process of two liquid threads of R^*=2, L^*=30, L_1^*=10, L_2^*=10, L_3^*=0, L_4^*=15

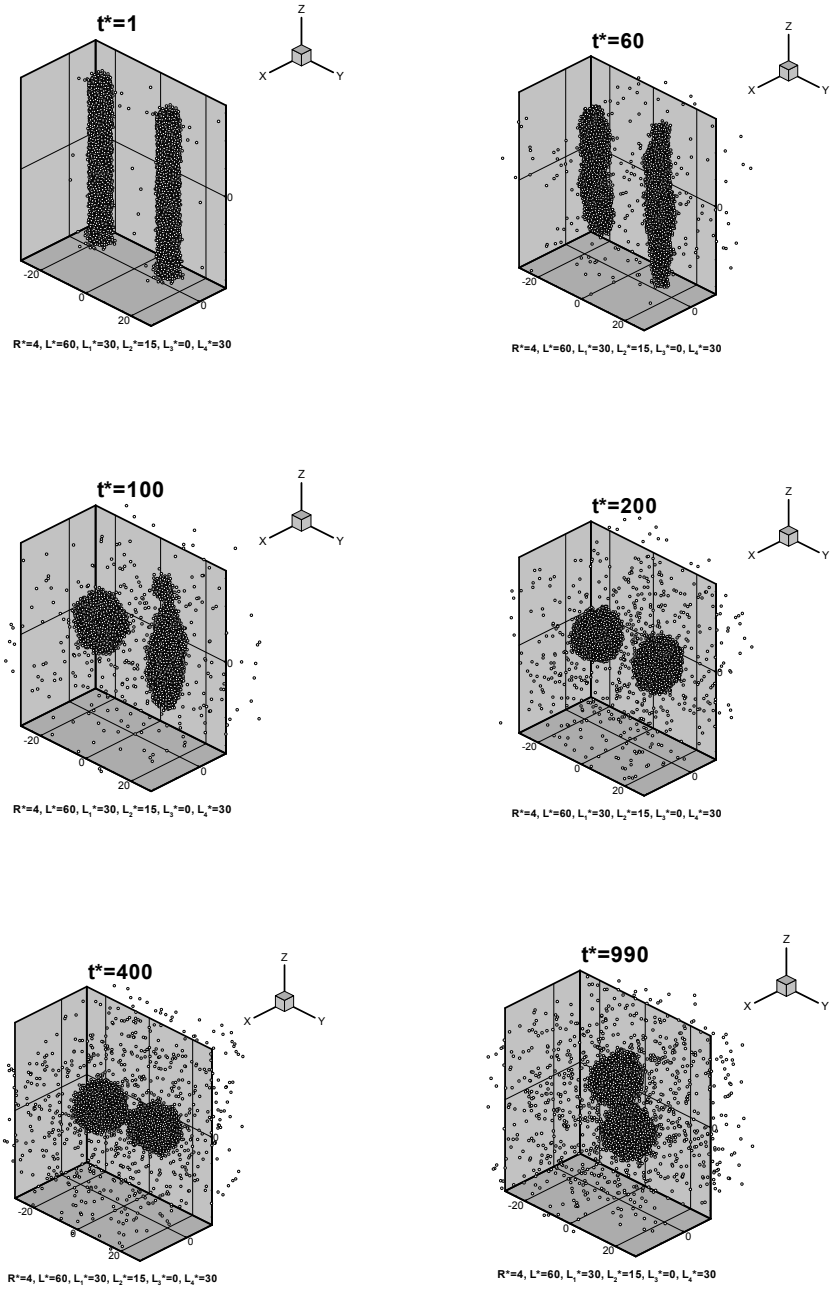

Figure 4: Vaporization process of two liquid threads of R^*=4, L^*=60, L_1^*=30, L_2^*=15, L_3^*=0, L_4^*=30

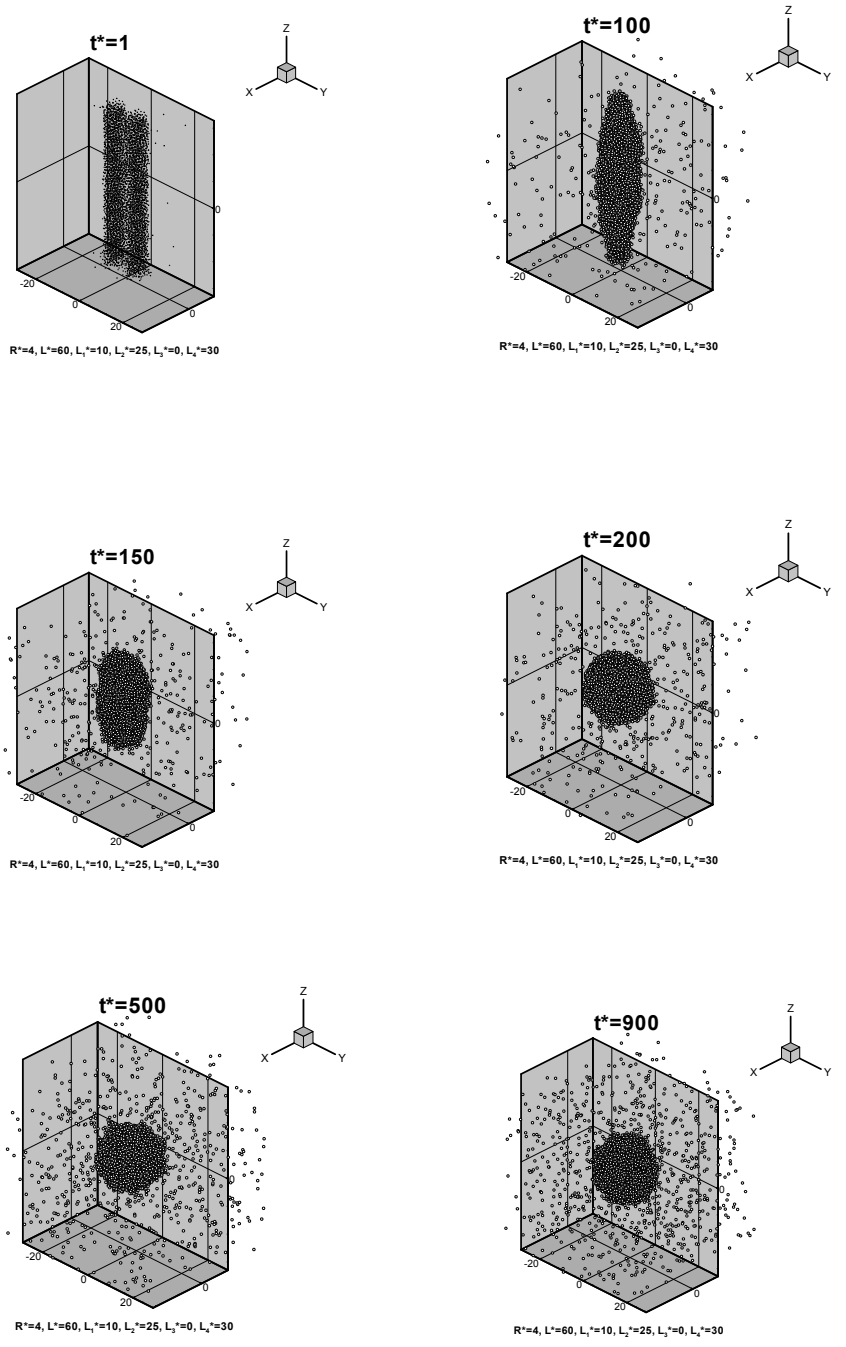

Figure 5: Vaporization process of two liquid threads of R^*=4, L^*=60, L_1^*=10, L_2^*=25, L_3^*=0, L_4^*=30

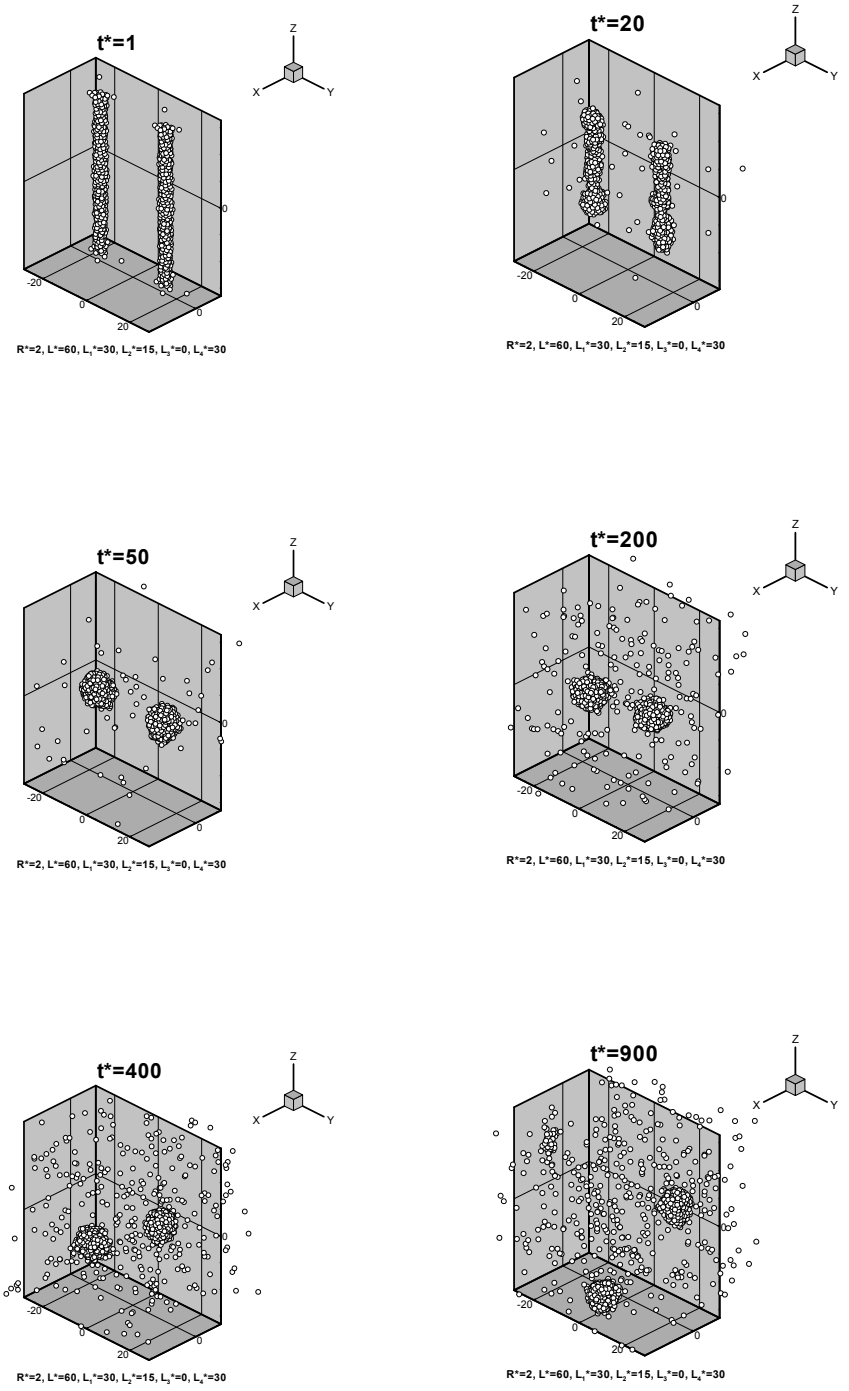

Figure 6: Vaporization process of two liquid threads of R^*=2, L^*=60, L_1^*=30, L_2^*=15, L_3^*=0, L_4^*=30

axial directions. Two liquid particles are formed and prevail during the subsequent vaporization process. For two closer liquid threads, e.g., R^*=2, L^*=60, L_1^*=10, L_2^*=25 and L_4^*=30 (case 7 in Table 1) , the vaporization process, which is shown in Fig.7, is different from case 6. The two threads also rupture from their two ends and get shorter due to the contraction motion in their axial directions. Two liquid particles are formed but they quickly coalesce into a single particle and prevail during the subsequent vaporization process. This vaporization process is similar to but slightly different from that for thicker liquid threads (case 4) . The thinner liquid threads (case 7) evolve into two liquid particles and then quickly coalesce into a single particle while the thicker liquid threads (case 4) quickly coalesce into a single liquid thread and then evolve into a single liquid particle.

From Table 1, it is seen that the value of $\overline{f_\rho}$ is larger for case 7, i.e., vaporization is slower when the two liquid threads are close to each other. In addition, Table 1 shows that more liquid particles are produced when the separation of the two threads is larger (case 6) . Case 8, which was investigated in our previous study (2009b), denotes the situation for a single liquid thread of the same radius and length as those in cases 6 and 7. From Table 1, it is seen that only one liquid particle is formed for case 8 and the vaporization speed for case 8 is slower than case 6, for which two liquid particles are formed. This corroborates the previous results for thicker liquid threads (cases 3, 4 and 5) . Furthermore, comparing cases 6$\sim$8 for thinner liquid threads (R^*=2) with cases 3$\sim$5 for thicker liquid threads (R^*=4) , it can be seen that the value of $\overline{f_\rho}$ is smaller for thinner liquid threads, which implies that thinner liquid threads evaporate more quickly. This also corroborates the previous results for shorter liquid threads (cases 1 and 2) .

Figure 8 shows the vaporization process of two liquid threads of R^*=4, L^*=120, L_1^*=60, L_2^*=30 and L_4^*=60 (case 9 in Table 1) . Similar to case 3 for shorter liquid threads, the two threads rupture from their two ends and get shorter due to the contraction motion in their axial directions. Two liquid particles are formed and prevail during the subsequent vaporization process. For two closer liquid threads, e.g., R^*=4, L^*=120, L_1^*=40, L_2^*=40 and L_4^*=60 (case 10 in Table 1) , the vaporization process, which is shown in Fig.9, is similar to case 9. Two liquid particles are formed and prevail during the subsequent vaporization process. If the two liquid threads get even closer, e.g., R^*=4, L^*=120, L_1^*=10, L_2^*=55 and L_4^*=60 (case 11 in Table 1) , the vaporization process, which is shown in Fig.10, is quite different from cases 9 and 10. Similar to case 4 for shorter liquid threads, it is observed that because the two threads in case 11 are very close to each other, they quickly coalesce into a single thread before they separately evolve into liquid particles. The coalesced liquid thread then gets shorter due to the contraction motion in its axial direction and finally evolves into a single liquid particle.

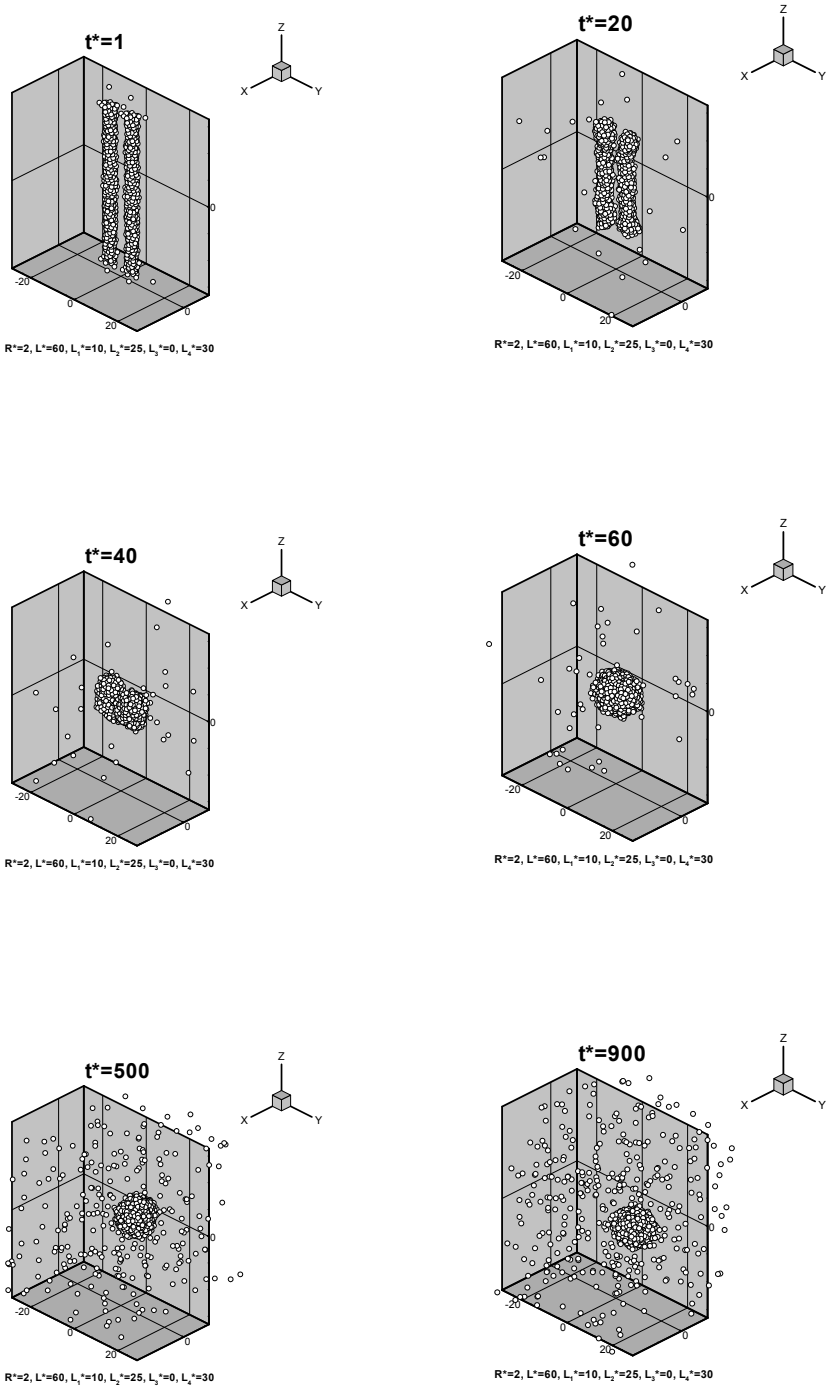

Figure 7: Vaporization process of two liquid threads of R^*=2, L^*=60, L_1^*=10, L_2^*=25, L_3^*=0, L_4^*=30

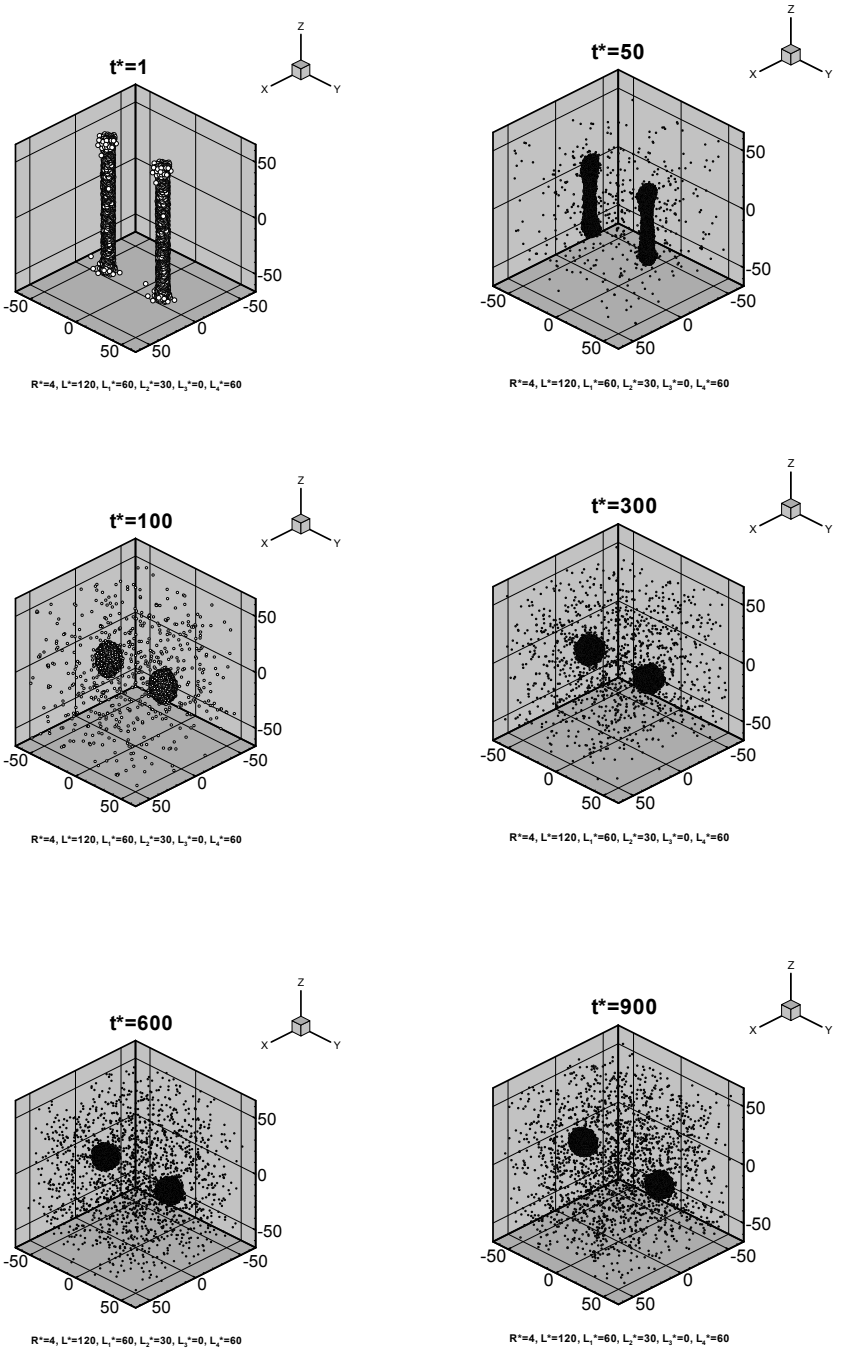

Figure 8: Vaporization process of two liquid threads of R^*=4, L^*=120, L_1^*=60, L_2^*=30, L_3^*=0, L_4^*=60

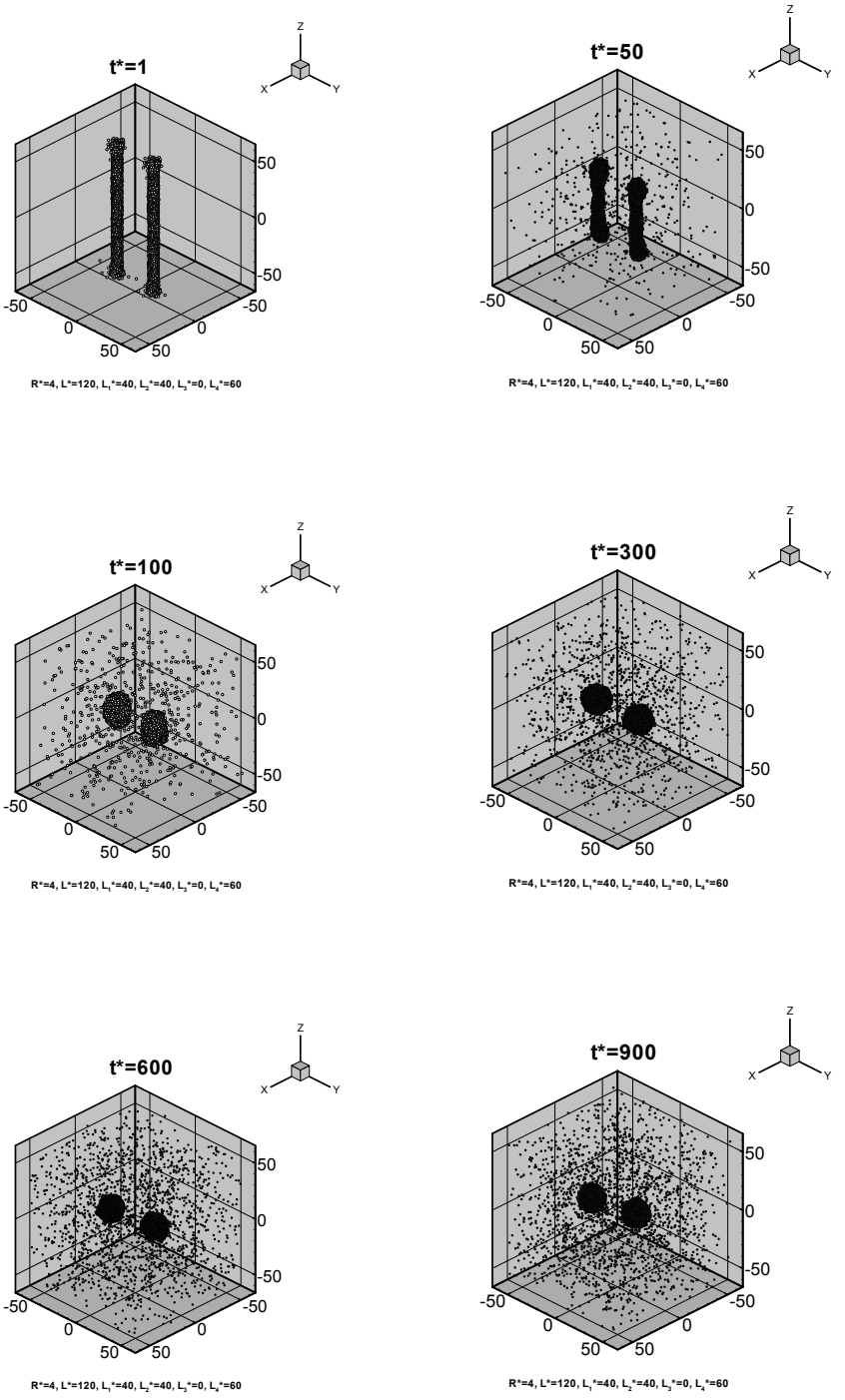

Figure 9: Vaporization process of two liquid threads of R^*=4, L^*=120, L_1^*=40, L_2^*=40, L_3^*=0, L_4^*=60

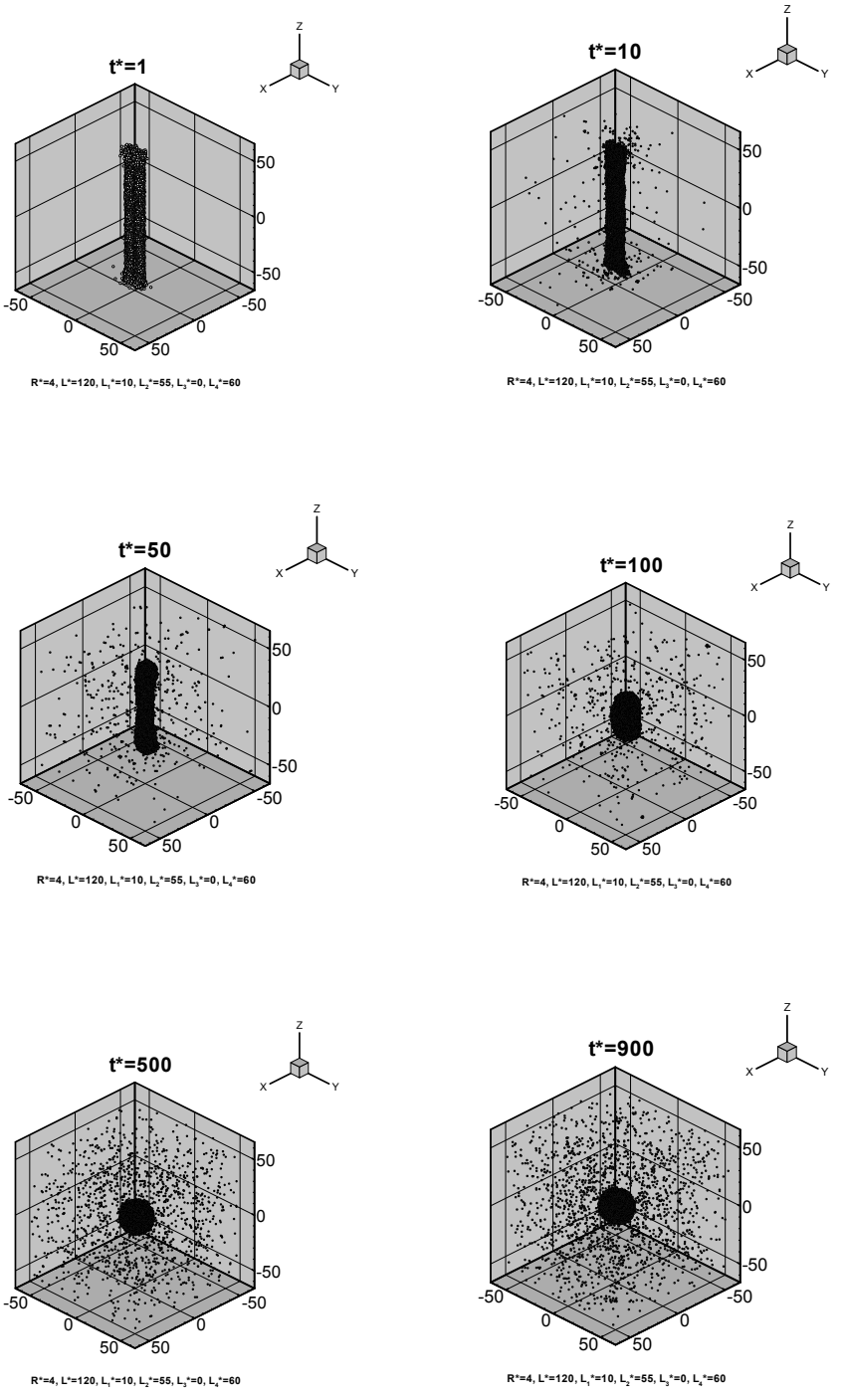

Figure 10: Vaporization process of two liquid threads of R^*=4, L^*=120, L_1^*=10, L_2^*=55, L_3^*=0, L_4^*=60

Similar to cases 4 and 7, Table 1 shows that the value of $\overline{f_\rho}$ is larger for case 11, i.e., vaporization is slower when the two liquid threads are very close to each other. Similarly, it is seen that more liquid particles are produced when the separation of the two threads is larger (cases 9 and 10) . Case 12, which was investigated in our previous study (2009b), denotes the situation for a single liquid thread of the same radius and length as those in cases 9∼11. From Table 1, it is seen that only one liquid particle is formed for case 12 and the vaporization speed for case 12 is slower than in cases 9 and 10, for which two liquid particles are formed. This corroborates the previous results for shorter liquid threads (cases 3∼8) .

Figure 11 shows the vaporization process of two liquid threads of R^*=2, L^*=120, L_1^*=60, L_2^*=30 and L_4^*=60 (case 13 in Table 1) . For this case of thinner liquid threads, it is seen that the two threads rupture from their two ends and quickly evolve into ten liquid particles. During the vaporization process, collision and coalescence of the liquid particles occur and finally two liquid particles are formed. For two closer liquid threads, e.g., R^*=2, L^*=120, L_1^*=40, L_2^*=40 and L_4^*=60 (case 14 in Table 1) , the vaporization process, which is shown in Fig.12, is similar to but slightly different from that of case 13. Nine liquid particles are formed initially and they finally evolve into two liquid particles by collision and coalescence. If the two liquid threads get even closer, e.g., R^*=2, L^*=120, L_1^*=10, L_2^*=55 and L_4^*=60 (case 15 in Table 1) , the vaporization process, which is shown in Fig.13, is different from those in cases 13 and 14. Nine liquid particles are formed, but they finally evolve into a single particle by collision and coalescence.

Similar to cases 4, 7 and 11, Table 1 shows that the value of $\overline{f_\rho}$ is larger for case 15, i.e., vaporization is slower when the two liquid threads are very close to each other. Similarly, it can also be seen that more liquid particles are formed when the separation of the two threads is larger (cases 13 and 14) . Case 16, which was investigated in our previous study (2009b), denotes the situation for a single liquid thread of the same radius and length as those in cases 13∼15. From Table 1, it is seen that less liquid particles are formed for case 16 and the vaporization speed for case 16 is slower than in cases 13 and 14, in which more liquid particles are formed. This corroborates the previous results (cases 3∼12) . Furthermore, comparing cases 13∼16 for thinner liquid threads (R^*=2) with cases 9∼12 for thicker liquid threads (R^*=4) , it is seen that the value of $\overline{f_\rho}$ is smaller for thinner liquid threads, which implies that thinner liquid threads evaporate more quickly. This also corroborates the previous results for shorter liquid threads (cases 1∼8) .

Figure 14 shows the vaporization process of two liquid threads of R^*=4, L^*=240, L_1^*=120, L_2^*=60 and L_4^*=120 (case 17 in Table 1) . Similar to cases 3 and 9 for shorter liquid threads, the two threads rupture from their two ends and get shorter due to the contraction motion in their axial directions. Two liquid particles are

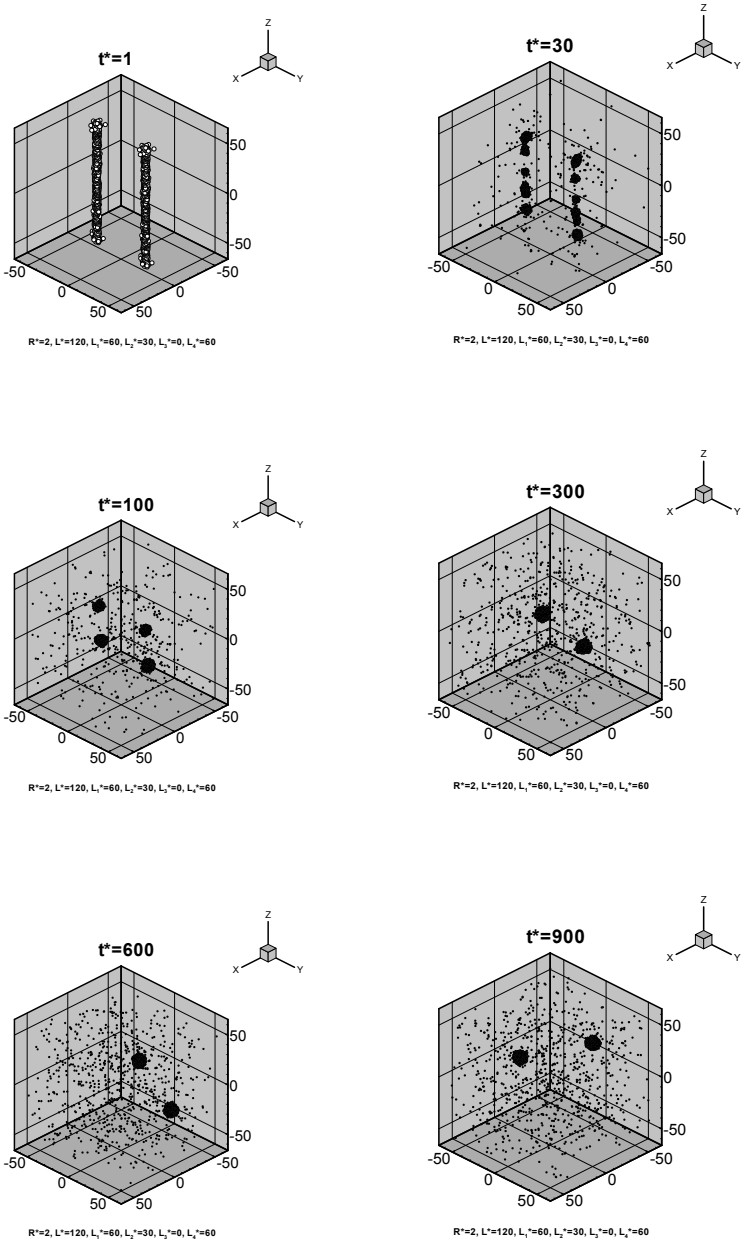

Figure 11: Vaporization process of two liquid threads of R^*=2, L^*=120, L_1^*=60, L_2^*=30, L_3^*=0, L_4^*=60

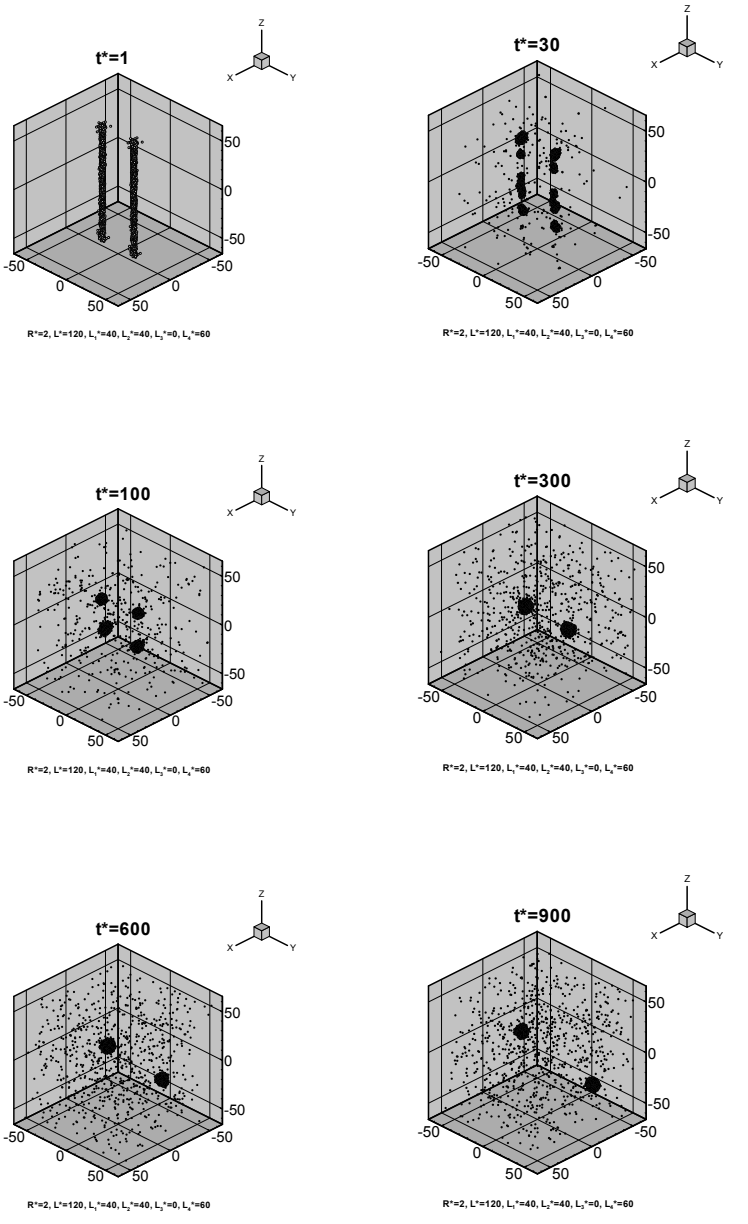

Figure 12: Vaporization process of two liquid threads of R^*=2, L^*=120, L_1^*=40, L_2^*=40, L_3^*=0, L_4^*=60

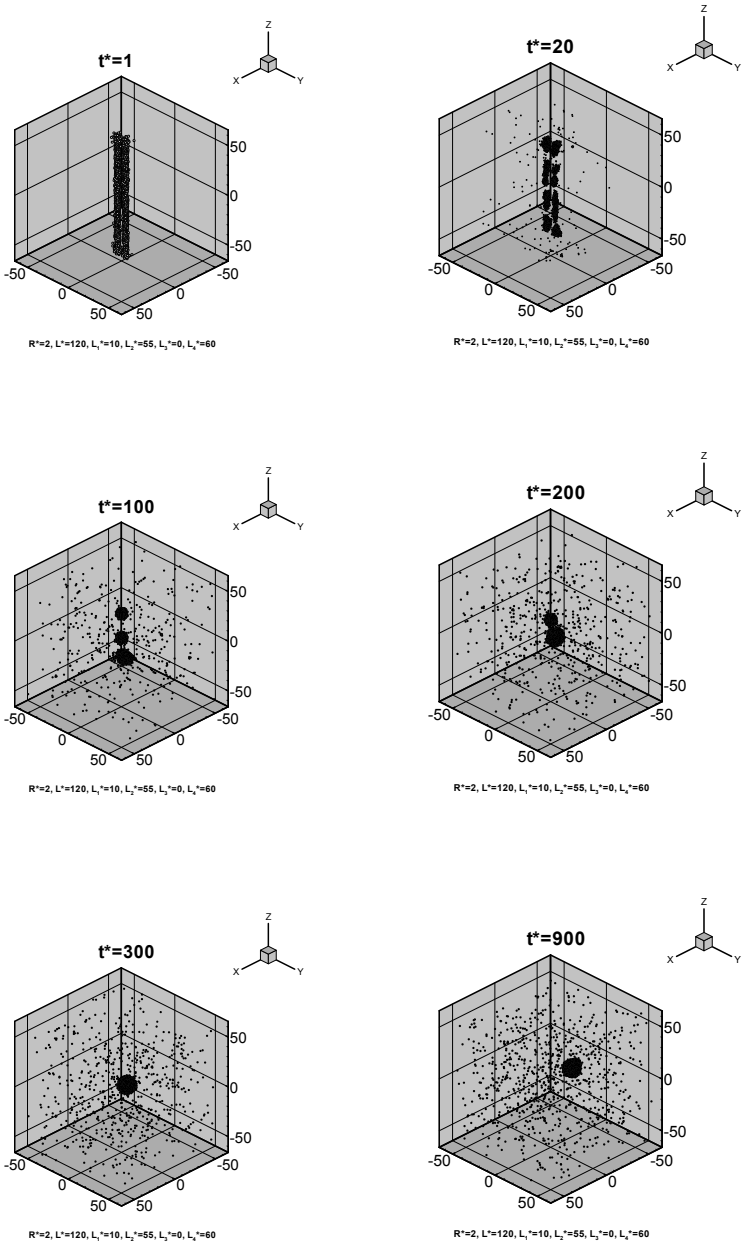

Figure 13: Vaporization process of two liquid threads of R^*=2, L^*=120, L_1^*=10, L_2^*=55, L_3^*=0, L_4^*=60

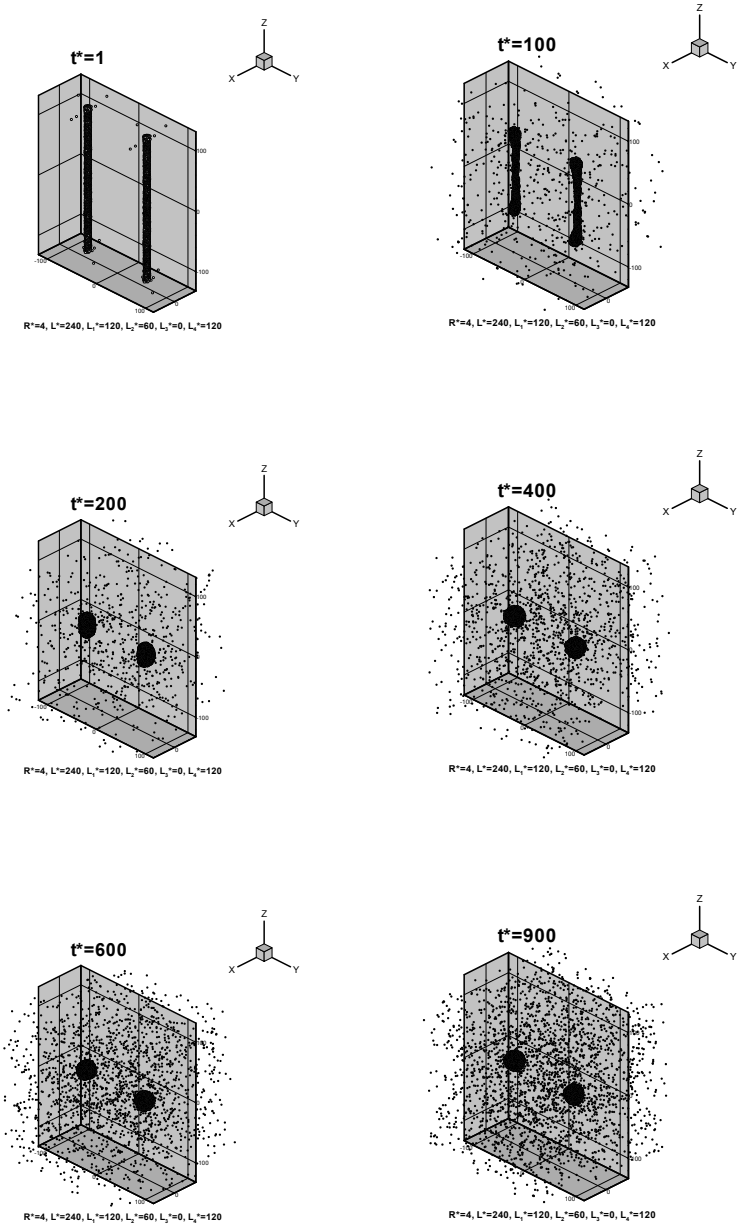

Figure 14: Vaporization process of two liquid threads of R^*=4, L^*=240, L_1^*=120, L_2^*=60, L_3^*=0, L_4^*=120

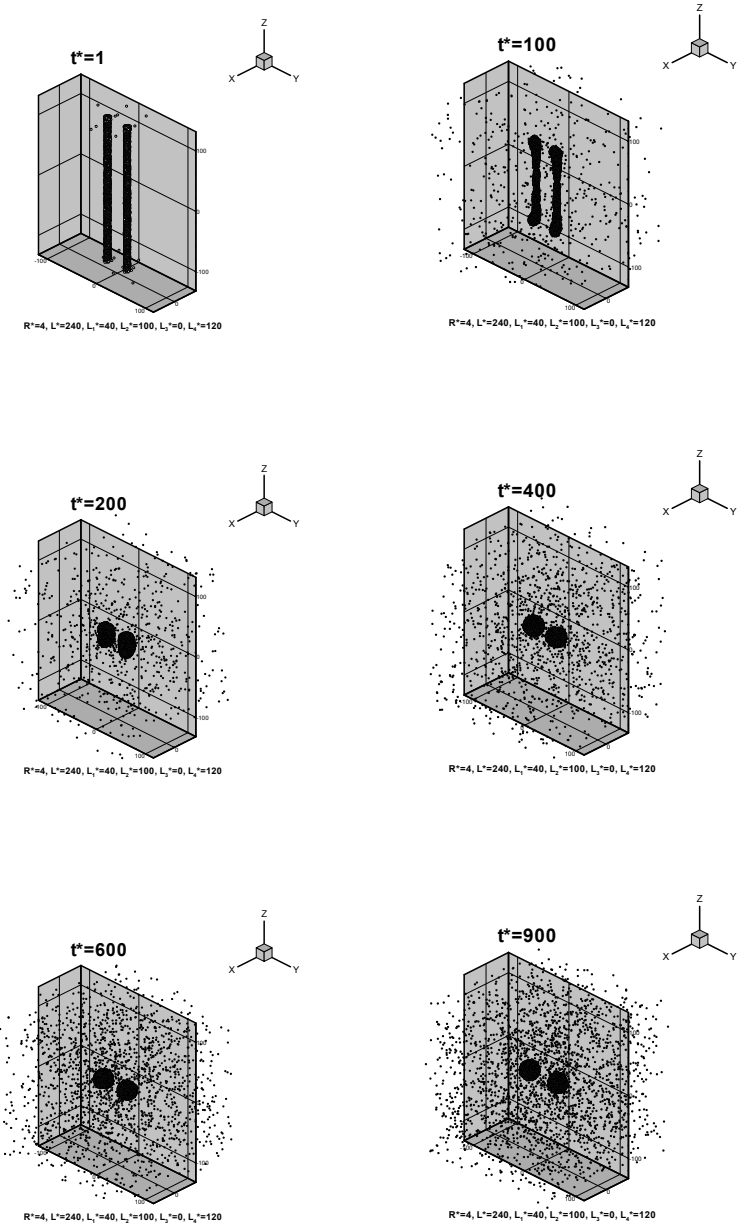

Figure 15: Vaporization process of two liquid threads of R^*=4, L^*=240, L_1^*=40, L_2^*=100, L_3^*=0, L_4^*=120

formed and prevail during the subsequent vaporization process. For two closer liquid threads, e.g., R^*=4, L^*=240, L_1^*=40, L_2^*=100 and L_4^*=120 (case 18 in Table 1) , the vaporization process, which is shown in Fig.15, is similar to that in case 17. If the two liquid threads get even closer, e.g., R^*=4, L^*=240, L_1^*=10, L_2^*=115 and L_4^*=120 (case 19 in Table 1) , the vaporization process, which is shown in Fig.16, is quite different from those in cases 17 and 18. Similar to cases 4 and 11 for shorter liquid threads, it is seen that because the two threads in case 19 are very close to each other, they quickly coalesce into a single thread before they separately evolve into liquid particles. The coalesced liquid thread then becomes shorter due to the contraction motion in its axial direction and finally evolves into a single liquid particle.

From Table 1, it is observed that the value of $\overline{f_\rho}$ is larger for case 19, i.e., vaporization is slower when the two liquid threads are very close to each other. Similarly, it can be seen that more liquid particles are produced when the separation of the two threads is larger (cases 17 and 18) . Case 20, which was investigated in our previous study (2009b), denotes the situation for a single liquid thread of the same radius and length as those in cases 17$\sim$19. From Table 1, it is seen that only one liquid particle is formed for case 20 and the vaporization speed for case 20 is slower than those in cases 17 and 18, for which two liquid particles are formed. This corroborates the previous results for shorter liquid threads (cases 3$\sim$16) .

If the length of the liquid thread is further increased, e.g. R^*=4 and L^*=480, more liquid particles are formed. Figure 17 shows the vaporization process of two liquid threads of R^*=4, L^*=480, L_1^*=160, L_2^*=160 and L_4^*=240 (case 21 in Table 1) . Eight liquid particles are formed and they evolve into four liquid particles by collision and coalescence. For two closer liquid threads, e.g., R^*=4, L^*=480, L_1^*=40, L_2^*=220 and L_4^*=240 (case 22 in Table 1) , the vaporization process, which is shown in Fig.18, is similar to but slightly different from that in case 21. Six liquid particles are formed initially and they finally evolve into two liquid particles by collision and coalescence. If the two liquid threads get even closer, e.g., R^*=4, L^*=480, L_1^*=10, L_2^*=235 and L_4^*=240 (case 23 in Table 1) , the vaporization process, which is shown in Fig.19, is very different from those in cases 21 and 22. Because the two threads in case 23 are very close to each other, they quickly coalesce into a single thread before they separately evolve into liquid particles. The coalesced liquid thread ruptures from its ends and interior and gets shorter due to the contraction motion in its axial direction and finally evolves into a single liquid particle by collision and coalescence. The vaporization process for case 23 (Fig.19) is similar to but slightly different from that in case 19 (Fig.16) . For both cases, the two threads quickly coalesce into a single thread because they are very close to each other. However, the coalesced liquid thread in case 19 evolves into a single liquid particle without

rupturing in its interior while the coalesced liquid thread for case 23 ruptures in its interior before it finally evolves into a single liquid particle.

From Table 1, it is observed that the value of $\overline{f_\rho}$ is larger for case 23, i.e., vaporization is slower when the two liquid threads are very close to each other. Similarly, it can be seen that more liquid particles are produced when the separation of the two threads is larger (cases 21 and 22) . Case 24, which was investigated in our previous study (2009b), denotes the situation for a single liquid thread of the same radius and length as those in cases 21∼23. From Table 1, it can be seen that less liquid particles are formed for case 24 and the vaporization speed for case 24 is slower than those in cases 21 and 22, in which more liquid particles are formed. This corroborates the previous results for shorter liquid threads (cases 3∼20) .

From the above discussion, the following observations can be made.

First, if the fundamental cell length is small, the liquid threads may remain intact or evolve into only one liquid particle in the cell. If the threads break up in this case, they rupture from their ends only, i.e. the top and bottom surfaces of the fundamental cell, but not from their interiors. On the other hand, if the fundamental cell length is larger, more than one liquid particle may be produced in the cell and the liquid threads may rupture not only from their ends but also from their interiors.

Second, thinner liquid threads may produce more liquid particles in the cell and evaporate more quickly.

Third, more liquid particles are formed when the separation of the two threads is larger. Moreover, vaporization is slower when the two liquid threads are close to each other.

Fourth, on the basis of identical liquid thread radius and length, liquid threads that produce more liquid particles evaporate more quickly.

3.2 Stability Analysis

In the scope of fluid flow research, instability has received a great deal of attention due to its potential influence on flow development. Previous instability analyses, e.g., Lord Rayleigh (1879), Weber (1931) and Tomotika (1935), have focused mainly on large scale flow fields. The applicabilities of these theories to micro- or nano-scale flow fields are still uncertain. On the other hand, previous instability analyses for nano-scale liquid threads, e.g., Koplik and Banavar (1993), Kawano (1998), Min and Wong (2006), Kim, Lee, Han and Park (2006) and Yeh (2009b) , have been devoted to the investigation of a single liquid thread in a periodic fundamental cell. Because of the interaction between the two nano-scale liquid threads coexisting in a periodic fundamental cell, the vaporization process is quite different from that of a single liquid thread. In the following discussion, two linear stability

criteria, namely Rayleigh's stability criterion (1879) and Kim's stability criterion (2006), are accessed for their validity in molecular scale. This is the first study to investigate the instability of two nano-scale liquid threads coexisting in a periodic fundamental cell by MD simulation.

According to classical theory by Rayleigh (1879), the radius of a liquid thread, R, is related to the critical wavelength of perturbation, λ_c , as

$$\lambda_c = 2\pi R \tag{5}$$

A liquid thread will break up into drops if the axial wavelength of the surface perturbation $L>\lambda_c$. If $L<\lambda_c$, the thread is stable and will remain intact. Owing to the periodic boundary conditions in this study, the fundamental cell size L^* can be regarded as the longest wavelength of the perturbation.

For R^*=2, λ_c^* is 12.6. According to Rayleigh's stability criterion, liquid threads of radius R^*=2 and length L^*=30, 60 and 120 are expected to be unstable and will break up into drop(s). From Figs.3, 6, 7, 11, 13 or Table 1 (cases 2, 6∼8, 13∼16) , Rayleigh's stability criterion holds for these cases.

For R^*=4, λ_c^* is 25.2. According to Rayleigh's stability criterion, liquid threads of radius R^*=4 and length L^*=30, 60, 120, 240 and 480 are expected to be unstable and will break up into drop(s). However, from Figs.2, 4, 5, 8∼10,14∼19 or Table 1 (cases 1, 3∼5, 9∼12, 17∼24) , the liquid threads of R^*=4 and L^*=30 (case 1) remain intact while the remaining liquid threads are unstable and break up into drop(s). Rayleigh's stability criterion violates the MD simulation result for case 1 but holds for the remaining cases. The invalidity of Rayleigh's stability criterion for case 1 can be interpreted according to the vaporization process shown in Fig.2. It is seen that the two liquid threads quickly coalesce into a single thread and remain intact. This is somewhat like combining the two threads to form a thread of a larger radius, which can increase the critical wavelength of perturbation, λ_c, according to Eq.(5) and, therefore, broaden the stable domain.

Recently, Kim, Lee, Han and Park (2006) proposed a new linear relation from their MD simulation results. From their study, Rayleigh's linear relation can be modified as

$$\lambda_c = 2.44\pi(R - 1.23) \tag{6}$$

From Eq.(6), λ_c^* for R^* of 2 and 4 are 5.9 and 21.2, respectively. Then, from Table 1, it is seen that Kim's stability criterion violates the MD simulation result for case 1 while it holds for the remaining cases. The validity of Kim's stability criterion is similar to that of Rayleigh's stability criterion.

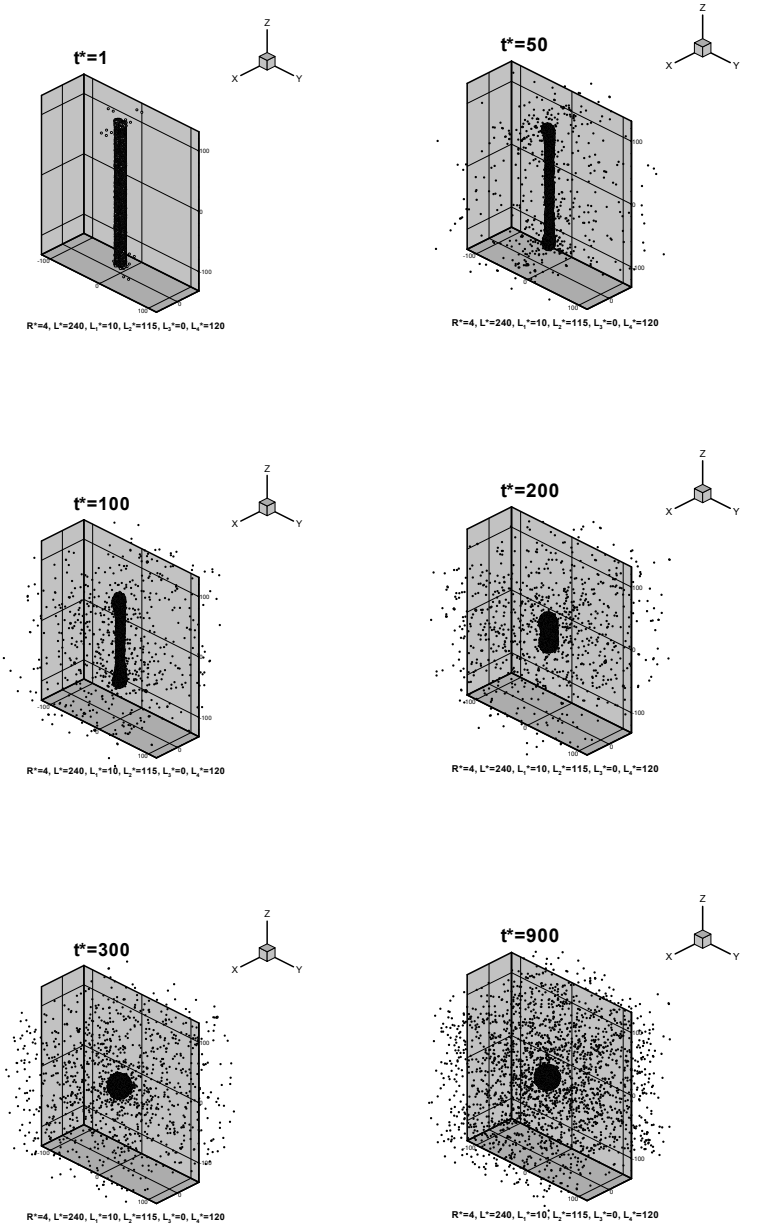

Figure 16: Vaporization process of two liquid threads of R^*=4, L^*=240, L_1^*=10, L_2^*=115, L_3^*=0, L_4^*=120

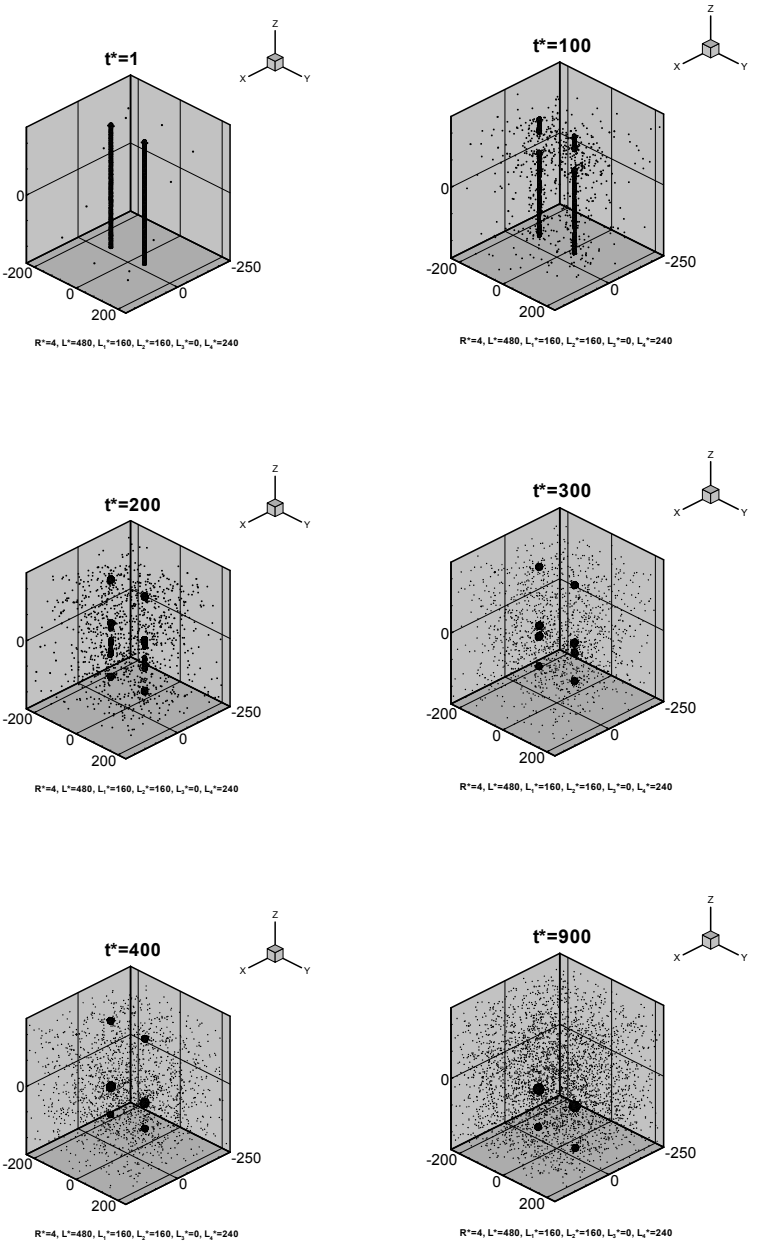

Figure 17: Vaporization process of two liquid threads of R^*=4, L^*=480, L_1^*=160, L_2^*=160, L_3^*=0, L_4^*=240

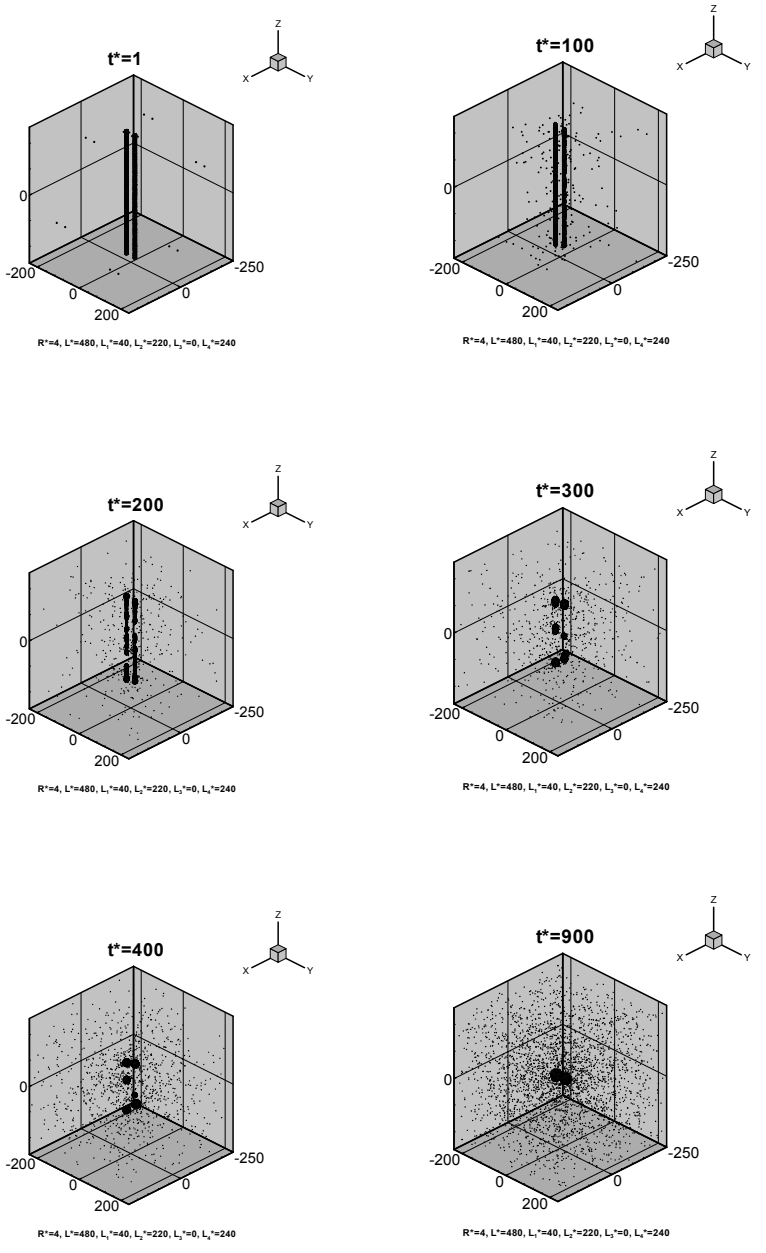

Figure 18: Vaporization process of two liquid threads of R^*=4, L^*=480, L_1^*=40, L_2^*=220, L_3^*=0, L_4^*=240

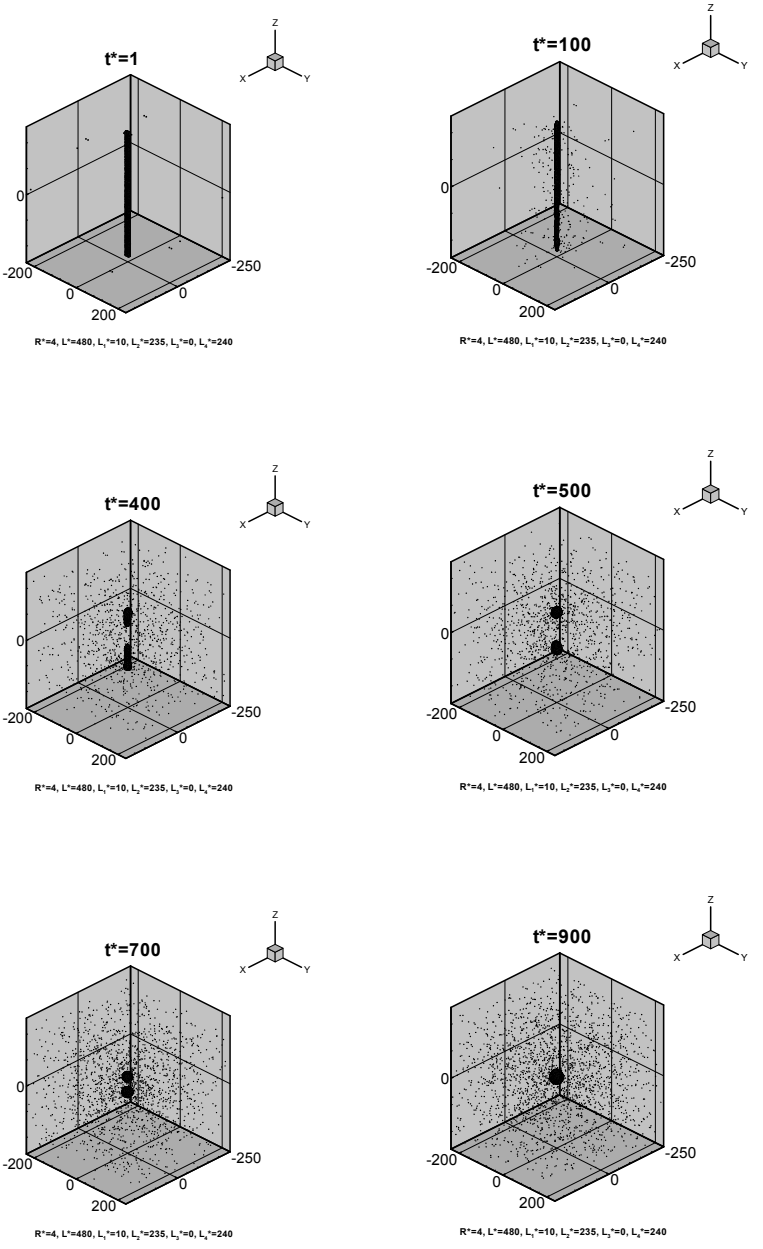

Figure 19: Vaporization process of two liquid threads of R^*=4, L^*=480, L_1^*=10, L_2^*=235, L_3^*=0, L_4^*=240

From the above discussion, it is found that the trends of Rayleigh's stability criterion and Kim's stability criterion agree with MD simulation results. However, when the two liquid threads coalesce into a single thread and remain intact, the critical wavelength of perturbation may be increased and the stable domain is broadened. In such a situation, Rayleigh's stability criterion and Kim's stability criterion underpredict the stable domain.

4 Conclusions

This study investigates the vaporization process of two nano-scale liquid threads coexisting in a periodic fundamental cell by MD simulation. The influences of liquid thread radius, fundamental cell length, and relative position of the two threads are discussed. Snapshots of molecules, number of liquid particles formed, and density field are analyzed. Two linear stability criteria, namely, Rayleigh's stability criterion and Kim's stability criterion, are accessed for their validity in molecular scale. It is found that the two liquid threads may remain intact or evolve into only one liquid particle if the fundamental cell length is small. If the threads break up in this case, they rupture from their ends only, i.e., the top and bottom surfaces of the fundamental cell, but not from their interiors. On the other hand, if the fundamental cell length is larger, more than one liquid particle may be produced in the cell and the liquid threads rupture not only from their ends but also from their interiors. It is also found that thinner liquid threads may produce more liquid particles in the cell and evaporate more quickly. In addition, more liquid particles are formed when the separation of the two threads is larger. Moreover, vaporization is slower when the two liquid threads are close to each other. On the basis of identical liquid thread radius and length, liquid threads that produce more liquid particles evaporate more quickly. Finally, the trends of Rayleigh's stability criterion and Kim's stability criterion agree with MD simulation results. However, when the two threads coalesce into a single one and remain intact, the critical wavelength of perturbation may be increased and the stable domain is broadened. In such a situation, Rayleigh's stability criterion and Kim's stability criterion underpredict the stable domain.

Acknowledgement: The author gratefully acknowledges the grant support from the National Science Council, Taiwan, R.O.C., under the contract NSC98-2221-E-150-041.

References

Chen, W. H.; Cheng, H. C.; Hsu, Y. C. (2007): Mechanical properties of carbon nanotubes using molecular dynamics simulations with the inlayer van der Waals

interactions. *CMES: Computer Modeling in Engineering & Sciences*, vol.20, no.2, pp.123-145.

Goren, S. (1962): The instability of an annular thread of fluid. *Journal of Fluid Mechanics*, vol.12, pp.309-319.

Haile, J. M. (1992): Molecular Dynamics Simulation. John Wiley & Sons, New York, chap.5.

Kawano, S. (1998): Molecular dynamics of rupture phenomena in a liquid thread. *Physical Review*, E, vol.58, no.4, pp.4468-4472.

Kim, B. G.; Lee, J. S.; Han, M.; Park, S. (2006): A molecular dynamics study on stability and thermophysical properties of nano-scale liquid threads. *Nano-scale and Micro-scale Thermophysical Engineering*, vol.10, pp.283-304.

Koplik, J.; Banavar, J. R. (1993): Molecular dynamics of interface rupture. *Physics of Fluids*, A, vol.5, no.3, pp.521-536.

Liu, D. S.; Tsai, C.Y. (2009): Estimation of thermo-elasto-plastic properties of thin-film mechanical properties using MD nanoindentation simulations and an inverse FEM/ANN computational scheme. *CMES: Computer Modeling in Engineering & Sciences*, vol.39, no.1, pp.29-48.

Lord Rayleigh (1879): On the stability of jets. *Proceedings of the London Mathematical Society*, vol.10, pp.4-13.

Matsumoto, R.; Nakagaki, M.; Nakatani, A.; Kitagawa, H. (2005): Molecular-dynamics study on crack growth behavior relevant to crystal nucleation in amorphous metal. *CMES: Computer Modeling in Engineering & Sciences*, vol.9, no.1, pp.75-84.

Min, D.; Wong, H. (2006): Rayleigh's instability of Lennard-Jones liquid nanothreads simulated by molecular dynamics. *Physics of Fluids*, vol.18, 024103.

Tomotika, S. (1935): On the instability of a cylindrical thread of a viscous liquid surrounded by another viscous liquid. *Proceedings of the Royal Society of London,* Series A, Mathematical and Physical Sciences, vol.150, no.870, pp.322-337.

Weber, C. (1931): Zum zerfall eines ussigkeitsstrahles. *Zeitschrift fur Angewandte Mathematik und Mechanik*. vol.11, no.2, pp.136-154.

Yeh, C. L. (2005): Turbulent flow investigation inside and outside plain-orifice atomizers with rounded orifice inlets. *Heat and Mass Transfer*, vol.41, no.9, pp.810-823.

Yeh, C. L. (2009a): Molecular dynamics simulation for the atomization process of a nanojet. *CMES: Computer Modeling in Engineering & Sciences*, vol.39, no.2, pp.179-200.

Yeh, C. L. (2009b): Molecular dynamics analysis of the instability for a nano-scale liquid thread. *CMES: Computer Modeling in Engineering & Sciences*, vol.50, no.3, pp.253-283.